Fermi National Accelerator Laboratory

Discovering a Light Higgs Boson with Light

Greg Landsberg and Konstantin T. Matchev

Fermi National Accelerator Laboratory
P.O. Box 500, Batavia, Illinois 60510

January 2000

Disclaimer

Distribution

Copyright Notification

Discovering a Light Higgs Boson with Light

Greg Landsberg[1] and Konstantin T. Matchev[2]

[1] *Physics Department, Brown University, 182 Hope St, Providence, RI 02912*
[2] *Theoretical Physics Department, Fermi National Accelerator Laboratory, Batavia, IL 60510*

Abstract. We evaluate the prospects for detecting a non-standard light Higgs boson with a significant branching ratio to two photons, in the Run II of the Fermilab Tevatron. We derive the reach for several channels: 2γ inclusive, $2\gamma + 1$ jet, and $2\gamma + 2$ jets. We present the expected Run II limits on the branching ratio of $h \to \gamma\gamma$ as a function of the Higgs mass, for the case of "bosonic", as well as "topcolor" Higgs bosons.

MOTIVATION

The Standard Model (SM) is very economical in the sense that the Higgs boson responsible for electroweak symmetry breaking can also be used to generate fermion masses. The Higgs boson couplings to the gauge bosons, quarks, and leptons are therefore predicted in the Standard Model, where one expects the Higgs boson to decay mostly to b-jets and tau pairs (for low Higgs masses, $m_h \lesssim 140$ GeV), or to WW or ZZ pairs, (for higher Higgs masses, $m_h \gtrsim 140$ GeV). Since the Higgs boson is neutral and does not couple to photons at tree level, the branching ratio $Br(h \to \gamma\gamma)$ is predicted to be very small in the SM, on the order of $10^{-3} - 10^{-4}$.

In a more general framework, however, where different sectors of the theory are responsible for the physics of flavor and electroweak symmetry breaking, one may expect deviations from the SM predictions, which may lead to drastic changes in the Higgs boson discovery signatures. One such example is the so called "fermiophobic" (also known as "bosophilic" or "bosonic") Higgs, which has suppressed couplings to all fermions. It may arise in a variety of models, see e.g. [1]. A variation on this theme is the Higgs in certain topcolor models, which may couple to heavy quarks only [2]. Some even more exotic possibilities have been suggested in the context of theories with large extra dimensions [3]. In all these cases, the Higgs boson decays to photon pairs are mediated through a W or heavy quark loop and dominate for $m_h \lesssim 100$ GeV [4]. In the range $100 \lesssim m_h \lesssim 160$, they compete with the WW^* mode, while for $m_h \gtrsim 160$ GeV, $h \to WW$ completely takes over. Existing bounds from LEP [5] are limited by the kinematic reach of the machine. Since $h \to \gamma\gamma$ is a very clean signature, it will allow the Tevatron to extend significantly those limits in its next runs.

In this study we shall evaluate the Higgs discovery potential of the upcoming Tevatron runs for several diphoton channels. We shall concentrate on the following two questions. First, what is the absolute reach in Higgs mass as a function of the $h \to \gamma\gamma$ branching ratio? Second, which signature (inclusive diphotons, diphotons plus one jet or diphotons plus two jets) provides the best reach. We believe that none of those two questions have been previously addressed in the literature.

TEVATRON REACH FOR A BOSONIC HIGGS

Here we consider the case of a "bosonic" Higgs, i.e. the Higgs couplings to all fermions are suppressed. Then, the main Higgs production modes at the Tevatron are associated Wh/Zh production, as well as WW/ZZ fusion. All of these processes have comparable rates [6], so it makes sense to consider an inclusive signature first [7].

Inclusive channel: analysis cuts

We use the following cuts for our inclusive study: two photons with $p_T(\gamma) > 20$ GeV and rapidity $|\eta(\gamma)| < 2$, motivated by the acceptance of the CDF or DØ detectors in Run II. Triggering on such a signature is trivial; both collaborations will have diphoton triggers that are nearly fully efficient with such offline cuts.

We assume 80% diphoton identification efficiency, which we apply to both the signal and background estimates on top of the kinematic and geometrical acceptance. Again, this efficiency is motivated by the CDF/DØ EM ID efficiency in Run I and is not likely to change in Run II.

Inclusive channel: background

The main backgrounds to the inclusive diphoton channel come from the QCD production of dijets, direct photons, and diphotons. In the former two cases a jet mimics a photon by fragmenting into a leading π^0/η meson that further decays into a pair of photons, not resolved in the calorimeter.

We used the PYTHIA [8] event generator and the experimentally measured probability of a jet to fake a photon to calculate all three components of the QCD background. While the faking probability depends significanlty on the particular photon ID cut, for this study we used a jet-faking-photon probability of 10^{-3}, independent of the jet E_T, typical for the DØ ID cuts [9,10]. This probability is expected to remain more or less the same in Run II. We used 80% ID efficiency for the pair of photons, and required the photons to be isolated from possible extra jets in the event. We accounted for the NLO corrections via a constant k-factor of 1.34.

Adding all background contributions, for the total background in the inclusive diphoton channel we obtain the following parametrization:

$$\frac{d\sigma}{dM_{\gamma\gamma}} = \left[p_3 + p_4 \left(\frac{M_{\gamma\gamma}}{1 \text{ GeV}} \right) + p_5 \left(\frac{M_{\gamma\gamma}}{1 \text{ GeV}} \right)^2 \right] \exp\left\{ p_1 + p_2 \left(\frac{M_{\gamma\gamma}}{1 \text{ GeV}} \right) \right\}, \tag{1}$$

where $p_1 = 8.347 \pm 0.041$, $p_2 = -0.02456 \pm 0.00018$, $p_3 = 0.9191 \pm 0.0093$, $p_4 = -0.006823 \pm 0.000036$ and $p_5 = 0.00001820 \pm 0.00000022$. The total background, as well as the individual contributions from $\gamma\gamma$, γj and jj production, are shown in Fig. 1. Additional SM sources of the background to inclusive diphotons include Drell-Yan production with both electrons misidentified as photons, $W\gamma\gamma$ production, etc. and are all negligible compared to the QCD background.

The absolute normalization of the background obtained by the method above agrees well with the actual background measured by CDF and DØ in the diphoton mode [7,10].

In Fig. 2 we show the 95% CL upper limit on the differential cross section after cuts $d(\varepsilon \times \sigma(\gamma\gamma + X))/dM_{\gamma\gamma}$ as a function of the diphoton mass, given the above background prediction (here ε is the product of the acceptance and all efficiencies). This limit represents 1.96σ sensitivity to a narrow signal when doing a counting experiment in 1 GeV diphoton mass bins. This plot can be used to obtain the sensitivity to any resonance decaying into two photons as follows. One first fixes the width of the mass window around the signal peak which is used in the analysis. Then one takes the average value of the 95% C.L. limit in $d\sigma/dM_{\gamma\gamma}$ across the mass window from Fig. 2 and multiplies it by $\sqrt{w/\text{GeV}}$, where w is the width of the mass window[1], to obtain the corresponding signal cross-section after cuts. Similar scaling could be used if one is interested in the 3σ or 5σ reach.

What is the optimum mass window cut?

When searching for narrow resonances in the presence of large backgrounds (B), the best sensitivity toward signal (S) is achieved by performing an unbinned maximum likelihood fit to the sum of the expected signal and background shapes. However, simple counting experiments give similar sensitivity if the size of the signal "window" is optimized. For narrow resonances the observed width is dominated by the instrumental effects, and is often Gaussian. The background in a narrow window centered on the assumed position of the signal peak could be treated as linear. Therefore, the Gaussian significance of the signal, $S/\sqrt{B}$, as a function of the window width, w, is given by:

---

[1] The square root enters the calculation since the significance is proportional to the background to the $-1/2$ power.
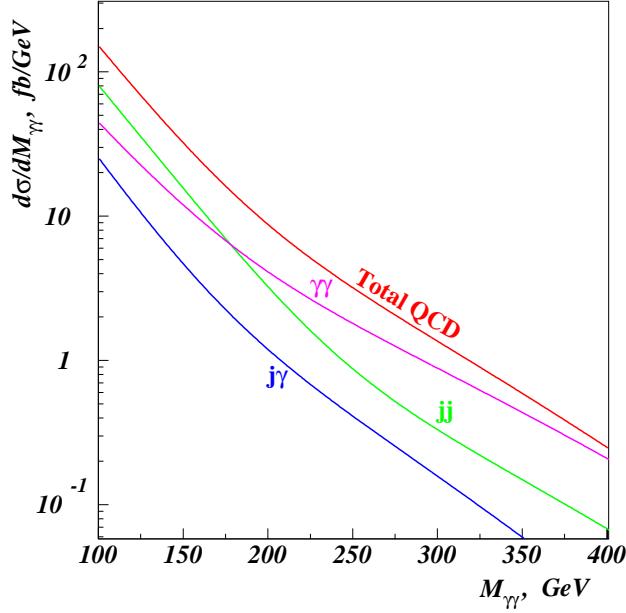
FIGURE 1. The total background in the inclusive diphoton channel, as well as the individual contributions from $\gamma\gamma$, γj and jj production.

$$S/\sqrt{B} \sim \mathrm{erf}(w)/\sqrt{w}, \tag{2}$$

where $\mathrm{erf}(x)$ is the error function. This function is shown in Fig. 3, and has a sharp maximum at $w \approx 1$, which corresponds to $\pm 1\sigma$ cut around the resonance maximum.

For resonances significantly wider than the experimental resoluton, the shape is given by the Breit-Wigner function, and in this case the significance is:

$$S/\sqrt{B} \sim \arctan(w)/\sqrt{w}. \tag{3}$$

This function, also shown in Fig. 3, peaks at a slightly higher value of w ($w \approx 1.4$), but the peak is broader than in the Gaussian case, and the significance does not appreciably deteriorate when using a $w = 1$ cut.

Therefore, in what follows we shall mostly use $\pm 1\sigma$ window centered on the resonance to obtain maximum sensitivity to the Higgs signal. Such an optimized choice of the window yields essentially the same significance as a full-blown unbinned likelihood shape fit. For the sake of comparison, however, we shall also present results for $\pm 2\sigma$ mass window cuts.

Inclusive channel: results

In Tables 1 and 2 we show the inclusive $\gamma\gamma + X$ background rates in fb for different Higgs masses, for 1σ and 2σ mass window cuts, respectively. Here we have added the intrinsic width and the experimental resolution $0.15\sqrt{2}\sqrt{E(\gamma)} \sim 0.15\sqrt{m_h}$ in quadrature. The two tables also show the significance for the inclusive diphoton channel when only associated Wh/Zh production and $WW/ZZ \to h$ fusion are included in the signal sample. We see that (as can also be anticipated from Fig. 3) a $\pm 1\sigma$ cut around the Higgs mass typically gives a better statistical significance, especially for lighter (and therefore more narrow) Higgs bosons.
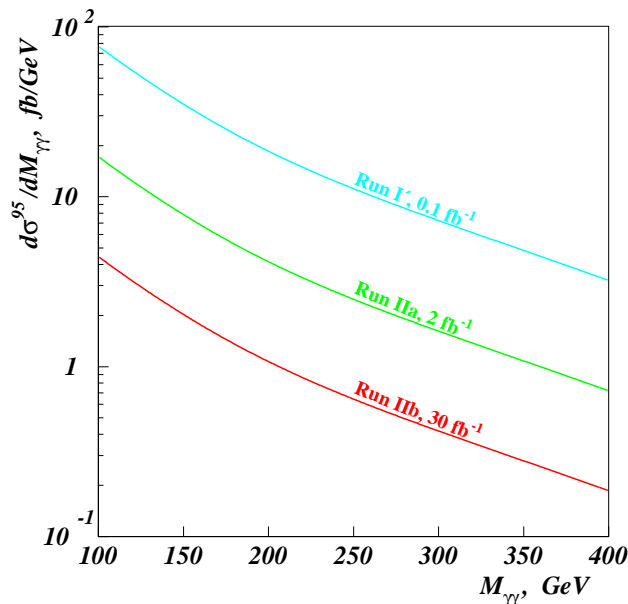
FIGURE 2. The 95% CL limit on $\varepsilon \times \sigma(\gamma\gamma + X)$ as a function of $M_{\gamma\gamma}$, for several benchmark total integrated luminosities in Run II. Here Run I' refers to 0.1 fb^{-1} at 2.0 TeV center-of-mass energy and Run II detectors.

Exclusive channels

The next question is whether the sensitivity can be further improved by requiring additional objects in the event. The point is that a significant fraction of the signal events from both associated Wh/Zh production and WW/ZZ fusion will have additional hard objects, most often QCD jets. In Fig. 4 we show the "jet" multiplicity in associated Wh production, where for detector simulation we have used the SHW package [11] with a few modifications as in [12]. Here we treat "jets" in a broader context, including electrons and tau jets as well.

Previous studies [7,13] have zoomed in on the case of associated production and required *two* or more additional QCD jets. Here we shall also consider the signature with at least *one* additional "jet", where a "jet" is an object with $|\eta| < 2$. The advantages of not requiring a second "jet" are twofold. First, in this way we can also pick up signal from $WW/ZZ \to h$ fusion, whose cross-section does not fall off as steeply with m_h, and in fact for $m_h > 200$ GeV is larger than the cross-section for associated Wh/Zh production[2]. Events from $WW/ZZ \to h$ fusion typically contain two very hard forward jets, one of which may easily pass the jet selection cuts. In Fig. 5 we show the pseudorapidity distribution of the two spectator jets in $WW/ZZ \to h$ fusion (red) and associated Wh/Zh production (blue). Second, by requiring only one additional jet, we win in signal acceptance. In order to compensate for the corresponding background increase, we shall consider several p_T thresholds for the additional jet, and choose the one giving the largest significance.

For the exclusive channels we need to rescale the background from Fig. 1 as follows. From Monte Carlo we obtain reduction factors of 4.6 ± 0.5, 6.2 ± 1.0 and 7.6 ± 1.4, for the $\gamma\gamma + 1$ jet channel, with $p_T(j) > 20$, 25 and 30 GeV, respectively. For the $\gamma\gamma + 2$ jets channel the corresponding background reduction is 21 ± 5, 38 ± 12 and 58 ± 21, depending on the jet p_T cuts. These scaling factors agree well with CDF and DØ data from Run I.

Notice that we choose not to impose an invariant dijet mass cut for the $\gamma\gamma + 2$ jets channel. We do not expect that it would lead to a gain in significance for several reasons. First, given the relatively high jet p_T cuts

---

[2] In the case of a topcolor Higgs (see the next section) we would also pick up events with initial state gluon radiation, comprising about 30% of the gluon fusion signal, which is the dominant production process for any Higgs mass.
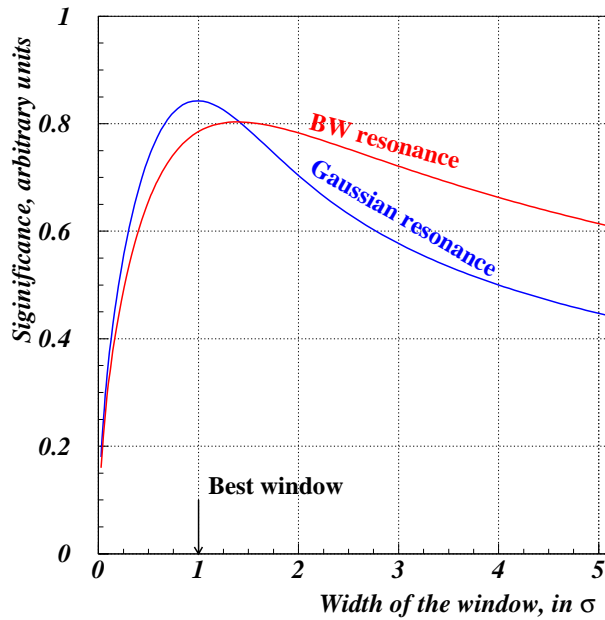
FIGURE 3. Significance $S/\sqrt{B}$, as a function of the mass window width, for a Gaussian or a Breit-Wigner resonance.

needed for the background suppression, there will be hardly any background events left with dijet invariant masses below the (very wide) W/Z mass window. Second, the signal events from WW/ZZ fusion, which typically comprise about $25-30\%$ of our signal, will have a dijet invariant mass distribution very similar to the background. And finally, this allows us to have a higher signal acceptance.

The significances for the two exclusive channels, with the three different jet p_T cuts, are also shown in Tables 1 and 2. We see that the exclusive $\gamma\gamma + 2$ jets channel with $p_T(j) > 30$ GeV typically gives the largest significance, but our new exclusive $\gamma\gamma + 1$ jet channel is following very close behind.

We are now ready to present our results for the Run II Tevatron reach for a bosonic Higgs. In Fig. 6 we show the 95% CL limit on the branching ratio $Br(h \to \gamma\gamma)$, with 0.1 (cyan), 2.0 (green) and 30 fb^{-1} (red), as a function of m_h. For each mass point, we compare the significance for both the inclusive as well as the exclusive channels with all the different cuts, and for the limit we choose the channel with the set of cuts providing the best reach. It turns out that for the case at hand the winners are: o: $2\gamma + 2j$, with $p_T(j) > 25$ GeV; □: $2\gamma + 2j$, with $p_T(j) > 30$ GeV and ◇: $2\gamma + 1j$, with $p_T(j) > 30$ GeV. In the figure we also show the HDECAY [14] prediction for $Br(h \to \gamma\gamma)$ in case of a "bosonic" Higgs. The reach shown for 0.1 fb^{-1} is intended as a comparison to Run I, in fact for the 0.1 fb^{-1} curve we scaled down both the signal and background cross-sections to their values at 1.8 TeV center-of-mass energy, keeping the efficiencies the same. In other words, the region marked as Run I' would have been the hypothetical reach in Run I, if the improved Run II detectors were available at that time.

TEVATRON REACH FOR A TOPCOLOR HIGGS

Here we consider the case of a "topcolor" Higgs [2], i.e. we include events from gluon fusion into our signal sample. We used the next-to-leading order cross-sections for gluon fusion from the HIGLU program [15].

In Tables 3 and 4 we show the significance in the inclusive and the two exclusive channels, for the topcolor Higgs case. Since gluon fusion, which rarely has additional hard jets, is the dominant production process, the inclusive channel typically provides the best reach. However, the $2\gamma + 1j$ channels are again very competitive, since the additional hard jet requirement manages to suppress the background at a reasonable signal cost.

TABLE 1. Background rates in fb for $\pm 1\sigma$ mass cut, and significance ($S/\sqrt{B}$), as a function of the Higgs mass m_h. The signal consists of associated Wh/Zh production and WW/ZZ fusion.

m_h (GeV)	$\gamma\gamma + X$ bknd (fb)	Significance $S/\sqrt{B}$						
		$\gamma\gamma + X$	$\gamma\gamma + 1$ jet			$\gamma\gamma + 2$ jets		
			$p_T(j) > 20$	$p_T(j) > 25$	$p_T(j) > 30$	$p_T(j) > 20$	$p_T(j) > 25$	$p_T(j) > 30$
100	454.7	11.1	20.9	23.2	24.5	22.3	25.9	24.6
120	256.8	9.0	16.9	18.7	19.8	17.3	20.4	19.5
140	156.4	7.0	13.0	14.4	15.5	13.6	15.5	16.4
160	92.4	6.0	11.2	12.6	13.2	11.4	13.4	14.0
180	59.8	4.6	8.6	9.6	10.3	8.6	10.3	10.4
200	43.9	3.8	7.0	7.9	8.5	7.1	8.3	8.9
250	30.0	2.1	3.8	4.3	4.7	3.7	4.5	4.8
300	24.0	1.2	2.1	2.3	2.5	2.0	2.5	2.8
350	18.3	0.7	1.2	1.3	1.4	1.0	1.3	1.4
400	14.3	0.4	0.6	0.7	0.8	0.5	0.6	0.7

In Fig. 7 we show the Run II reach for the branching ratio $Br(h \to \gamma\gamma)$ as a function of the Higgs mass, for the case of a "topcolor" Higgs boson.

CONCLUSIONS

We have studied the Tevatron reach for Higgs bosons decaying into photon pairs. For purely bosonic Higgses, which only couple to gauge bosons, the $2\gamma + 2j$ channel offers the best reach, but the $2\gamma + 1j$ channel is almost as good. For topcolor Higgs bosons, which can also be produced via gluon fusion, the inclusive $2\gamma + X$ channel is the best, but the $2\gamma + 1j$ channel is again very competitive. We see that in both cases the $2\gamma + 1j$ channel is a no-lose option!

REFERENCES

1. H. E. Haber, G. L. Kane and T. Sterling, "The Fermion Mass Scale And Possible Effects Of Higgs Bosons On Experimental Observables," Nucl. Phys. **B161**, 493 (1979); J. F. Gunion, R. Vega and J. Wudka, "Higgs Triplets In The Standard Model," Phys. Rev. **D42**, 1673 (1990); J. L. Basdevant, E. L. Berger, D. Dicus, C. Kao and S. Willenbrock, "Final state interaction of longitudinal vector bosons," Phys. Lett. **B313**, 402 (1993), hep-ph/9211225; V. Barger, N. G. Deshpande, J. L. Hewett and T. G. Rizzo, "A separate Higgs," preprint OITS-499, hep-ph/9211234; P. Bamert and Z. Kunszt, "Gauge boson masses dominantly generated by Higgs triplet contributions?," Phys. Lett. **B306**, 335 (1993), hep-ph/9303239. A. G. Akeroyd, "Fermiophobic Higgs bosons at the Tevatron," Phys. Lett. **B368**, 89 (1996), hep-ph/9511347; M. C. Gonzalez-Garcia, S. M. Lietti and S. F. Novaes, "Search for non-standard Higgs boson in diphoton events at $p\bar{p}$ collisions," Phys. Rev. **D57**, 7045 (1998), hep-ph/9711446; A. Barroso, L. Brucher and R. Santos, "Is there a light fermiophobic Higgs?," Phys. Rev. **D60**, 035005 (1999), hep-ph/9901293; L. Brucher and R. Santos, "Experimental signatures of fermiophobic Higgs bosons," hep-ph/9907434.
2. B. Dobrescu, "Minimal composite Higgs model with light bosons," preprint FERMILAB-PUB-99/234-T, hep-ph/9908391; B. Dobrescu, G. Landsberg and K. Matchev, preprint FERMILAB-PUB-99/324-T.

TABLE 2. The same as Table 1, but for a $\pm 2\sigma$ mass window.

m_h (GeV)	$\gamma\gamma + X$ bknd (fb)	Significance $S/\sqrt{B}$						
		$\gamma\gamma + X$	$\gamma\gamma + 1$ jet			$\gamma\gamma + 2$ jets		
			$p_T(j) > 20$	$p_T(j) > 25$	$p_T(j) > 30$	$p_T(j) > 20$	$p_T(j) > 25$	$p_T(j) > 30$
100	910.5	10.3	19.3	21.5	22.9	20.2	23.2	23.1
120	514.4	8.5	15.8	17.6	18.6	16.1	18.3	18.6
140	313.3	6.6	12.2	13.7	14.7	12.8	14.8	15.1
160	185.2	5.8	10.8	12.1	12.8	11.0	13.0	13.7
180	119.8	4.6	8.6	9.6	10.2	8.5	9.8	10.5
200	87.9	3.7	6.7	7.5	8.1	6.6	7.8	8.2
250	60.3	1.9	3.5	3.9	4.2	3.4	4.1	4.5
300	48.5	1.0	1.8	2.0	2.1	1.7	2.1	2.3
350	37.8	0.5	1.0	1.0	1.1	0.8	1.1	1.1
400	31.7	0.3	0.5	0.6	0.6	0.4	0.5	0.6

3. L. Hall and C. Kolda, "Electroweak symmetry breaking and large extra dimensions," Phys. Lett. **B459**, 213 (1999), hep-ph/9904236; H. Cheng, B. A. Dobrescu and C. T. Hill, "Electroweak symmetry breaking and extra dimensions," preprint FERMILAB-PUB-99/358-T, hep-ph/9912343.

4. A. Stange, W. Marciano and S. Willenbrock, "Higgs bosons at the Fermilab Tevatron," Phys. Rev. **D49**, 1354 (1994), hep-ph/9309294; M. A. Diaz and T. J. Weiler, "Decays of a fermiophobic Higgs," preprint VAND-TH-94-1, hep-ph/9401259.

5. G. Abbiendi *et al.* [OPAL Collaboration], "Search for Higgs bosons and other massive states decaying into two photons in e^+e^- collisions at 189 GeV," Phys. Lett. **B464**, 311 (1999), hep-ex/9907060; K. Ackerstaff *et al.* [OPAL Collaboration], "Search for Higgs bosons and new particles decaying into two photons at $\sqrt{s} = 183$ GeV," Phys. Lett. **B437**, 218 (1998), hep-ex/9808014.

6. M. Spira, "Higgs boson production and decay at the Tevatron," preprint DESY-98-159, hep-ph/9810289.

7. P. J. Wilson [CDF collaboration], "Search for high mass photon pairs in $p\bar{p}$ collisions at $\sqrt{s} = 1.8$ TeV," FERMILAB-CONF-98-213-E *Contributed to 29th International Conference on High-Energy Physics (ICHEP 98), Vancouver, Canada, 23-29 Jul 1998.*

8. T. Sjöstrand, Comp. Phys. Comm. **82**, 74 (1994). We used version 6.136.

9. S. Abachi *et al.* [D0 Collaboration], "Studies of gauge boson pair production and trilinear couplings," Phys. Rev. **D56**, 6742 (1997), hep-ex/9704004, and references therein.

10. B. Abbott *et al.* [D0 Collaboration], "A search for heavy pointlike Dirac monopoles," Phys. Rev. Lett. **81**, 524 (1998), hep-ex/9803023.

11. J. Conway, talk given at the SUSY/Higgs Workshop meeting, Fermilab, May 14-16, 1998, additional information available at www.physics.rutgers.edu/jconway/soft/shw/shw.html.

12. J. D. Lykken and K. T. Matchev, "Supersymmetry signatures with tau jets at the Tevatron," Phys. Rev. **D61**, 015001 (2000), hep-ph/9903238; K. T. Matchev and D. M. Pierce, "Supersymmetry reach of the Tevatron via trilepton, like-sign dilepton and dilepton plus tau jet signatures," Phys. Rev. **D60**, 075004 (1999), hep-ph/9904282.

13. B. Abbott *et al.* [D0 Collaboration], "Search for nonstandard Higgs bosons using high mass photon pairs in $p\bar{p} \to \gamma\gamma + 2$ jets at $\sqrt{s} = 1.8$ TeV," Phys. Rev. Lett. **82**, 2244 (1999), hep-ex/9811029; J. Womersley, "Searches for new particles in photon final states at the Tevatron," preprint FERMILAB-CONF-97-380-E, *To be published in the proceedings of International Eurphysics Conference on High-Energy Physics (HEP 97), Jerusalem, Israel, 19-26 Aug 1997.*

14. A. Djouadi, J. Kalinowski and M. Spira, "HDECAY: A program for Higgs boson decays in the standard model and its supersymmetric extension," Comput. Phys. Commun. **108**, 56 (1998), hep-ph/9704448.

15. M. Spira, "HIGLU: A Program for the Calculation of the Total Higgs Production Cross Section at Hadron Colliders via Gluon Fusion including QCD Corrections," preprint DESY-T-95-05, hep-ph/9510347.
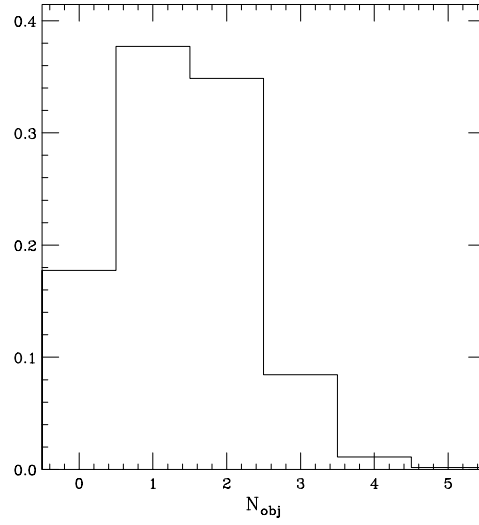
FIGURE 4. The number of "jets", which stands for QCD jets, tau jets and electrons, in associated Wh production, once we require the two photons from the Higgs to pass the photon ID cuts.
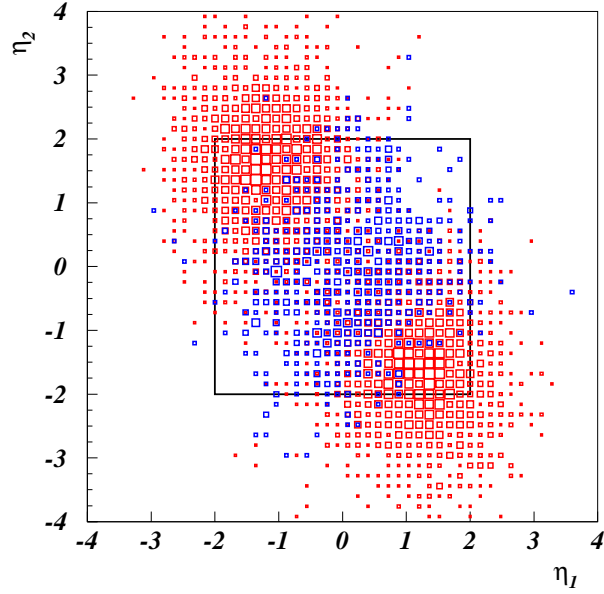

FIGURE 5. Pseudorapidity distribution of the two spectator jets in $WW/ZZ \to h$ fusion (red) and associated Wh/Zh production (blue). The boxed region represents the off-line selection cuts.
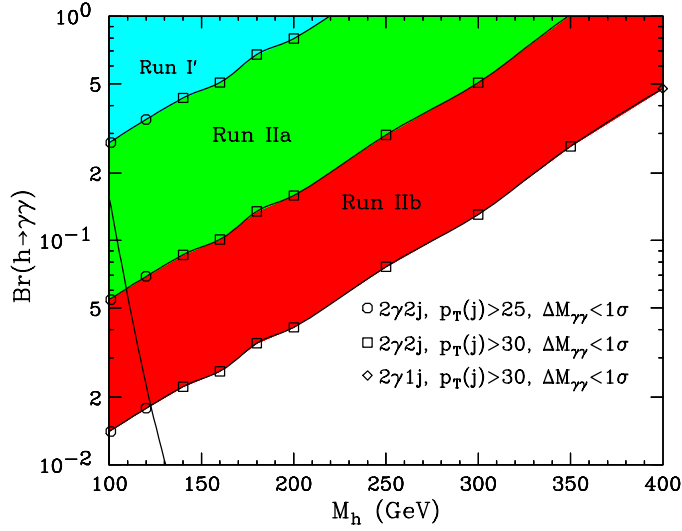
FIGURE 6. 95% CL limit on the branching ratio $Br(h \to \gamma\gamma)$, with 0.1 (cyan), 2.0 (green) and 30 fb^{-1} (red), as a function of m_h. For each mass point, we compare the significance for both the inclusive and the exclusive channels with different cuts, and for the limit we choose the set of cuts which provides the best reach - o: $2\gamma + 2j$, with $p_T(j) > 25$ GeV; □: $2\gamma + 2j$, with $p_T(j) > 30$ GeV and ◇: $2\gamma + 1j$, with $p_T(j) > 30$ GeV. The solid line is the prediction for the branching ratio of a "bosonic" Higgs.

TABLE 3. The same as Table 1, but for a topcolor Higgs, i.e. gluon fusion events are included in the signal.

m_h	$\gamma\gamma + X$ bknd	Significance $S/\sqrt{B}$						
		$\gamma\gamma + X$	$\gamma\gamma + 1$ jet			$\gamma\gamma + 2$ jets		
(GeV)	(fb)		$p_T(j) > 20$	$p_T(j) > 25$	$p_T(j) > 30$	$p_T(j) > 20$	$p_T(j) > 25$	$p_T(j) > 30$
100	454.7	34.8	28.7	29.8	30.2	23.4	27.1	25.6
120	256.8	28.8	25.0	26.4	26.7	18.6	21.6	20.6
140	156.4	23.3	20.2	21.3	22.0	14.8	16.7	17.5
160	92.4	20.1	18.0	19.4	19.6	13.0	15.1	15.3
180	59.8	16.2	14.6	15.4	15.6	10.2	11.9	11.7
200	43.9	13.4	12.4	13.0	13.5	8.3	9.5	10.0
250	30.0	8.1	7.6	8.1	8.2	4.5	5.3	5.6
300	24.0	5.0	4.6	4.9	4.9	2.7	3.3	3.4
350	18.3	3.7	3.4	3.6	3.6	1.7	2.0	2.0
400	14.3	2.4	2.2	2.3	2.4	1.0	1.1	1.1

TABLE 4. The same as Table 3, but for a $\pm 2\sigma$ mass window.

| m_h (GeV)	$\gamma\gamma + X$ bknd (fb)	Significance $S/\sqrt{B}$						
		$\gamma\gamma + X$	$\gamma\gamma + 1$ jet			$\gamma\gamma + 2$ jets		
			$p_T(j) > 20$	$p_T(j) > 25$	$p_T(j) > 30$	$p_T(j) > 20$	$p_T(j) > 25$	$p_T(j) > 30$
100	910.5	33.5	26.6	27.7	28.3	21.1	24.0	23.9
120	514.4	27.4	23.3	24.6	24.8	17.4	19.4	19.6
140	313.3	22.3	19.2	20.1	20.7	14.0	15.9	16.2
160	185.2	19.7	17.4	18.6	18.9	12.4	14.7	14.8
180	119.8	16.0	14.2	15.0	15.3	10.0	11.2	11.6
200	87.9	13.1	12.0	12.5	12.9	7.8	8.9	9.2
250	60.3	7.3	6.8	7.2	7.4	4.2	4.8	5.2
300	48.5	4.2	4.0	4.2	4.2	2.3	2.7	2.8
350	37.8	3.1	2.8	3.0	3.0	1.4	1.6	1.7
400	31.7	2.0	1.8	1.9	1.9	0.8	0.9	0.9
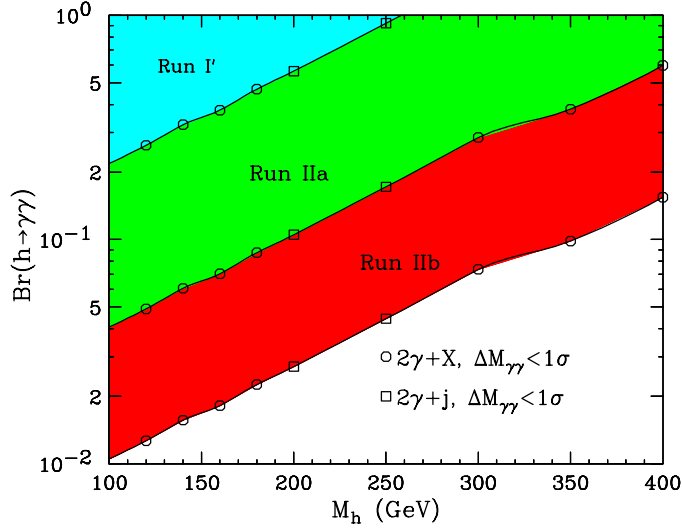
FIGURE 7. The same as Fig. 6, but for a topcolor Higgs, i.e. gluon fusion events are included in the signal.